DUBBLE-II Project

Conceptual Design Report for the

Small/Wide Angle Scattering BEAMLINE (BM26)

December 2016

DUBBLE-SAX-CDR-2016-001

Prepared by

Roelof van Silfhout

With input from

Reviewers and Approvals

Document Updates

Acknowledgements

Executive Summary

A concept for a SAXS/WAXS beamline is presented as a successor of the current BM26B facility. The beamline will serve the Dutch and Flemish users for the next 10 years once the upgraded ESRF synchrotron radiation source resumes operations in 2020.

The proposed design has the emphasis on ease of operation and flexibility in terms of complementary techniques that enable comprehensive studies of samples in both dynamic as static environments. With the significant beam size reduction, the new beamline is well positioned to allow users to investigate samples with high-spatial resolution. Although the source intensity is similar, changes in the beamline optics will result in a flux density increase at the sample for typical experiments. For experiments using small beams the flux density increase is significant. It is envisaged that due to this flexibility the proposed beamline supports experiments that are not limited to SAXS/WAXS due to the ease by which the beam size is varied at the sample position, of changing wavelength, sample environment and detector configuration.

Due to the high-quality source and refined focusing optics, the proposed beamline provides an excellent microprobe for many experiments regarding long and short-range order and do so with high spatial and temporal resolution. The little used high-precision diffractometer will be relocated to the sample position and modified such that it can act as a flexible sample stage for many experiments and improving conditions for grazing incidence studies. The detector arm provides a flexible base for a dedicated large angle detector option.

Overall the optical layout of the SAXS/WAXS beam line should be revised to make full use of the upgraded source. A collimating mirror will be introduced up stream of the monochromator. This will serve two purposes: first it will reduce the heat load on the monochromator by filtering the incident white beam and second the vertical divergence of the beam will be set close to zero. The sagittal focusing monochromator will be replaced the first phase of replacing the old system will be completed in Jan. 2018 with a complete overhaul of the crystal cage. The second phase will involve replacing the monochromator support and sagittal crystal and its bender as outlined in this report.

The existing optics hutch will provide plenty of space to add further optical components. For example, the use of compound refractive elements will benefit significantly from the increased brilliance. The higher coherent fraction will enable extend beamline capability with crossover experiments from coherent SAXS to ptychographic imaging. Smaller beam sizes will allow higher resolution using sample scanning (micro SAXS/WAXS) or the use of rasterising scans of radiation sensitive samples.

The addition of a Laue monochromator in transmission mode using a weakly absorbing monochromator crystal such as diamond provides the existing EXAFS experiments hutch with radiation suitable to conduct experiments at a semi-fixed wavelength. Depending on the exact configuration, this station would receive radiation from 15-45 keV making it suitable for a wide range of experiments. Due to the nature of the side-bounce monochromator this station would be primarily for static wavelength operation but a modest scan range can be provided if and when required.

Table of contents

Glossary

2PW - 2 Pole Wiggler

3PW - 3-pole Wiggler

BM26A/B - Existing DUBBLE beamlines A (spectroscopy) & B (SAXS)

BW - Band Width

CRG - Collaborative Research Group

CXDI - Coherent X-ray Diffraction Imaging

DCM - Double Crystal Monochromator

ESRF - European Synchrotron Radiation Facility

FE - Finite Element

SAXS - Small Angle X-ray Scattering

SBM - Short Bend Magnet

SR - Synchrotron Radiation

SRW - Synchrotron Radiation Workshop

VFM - Vertically Focusing Mirror

VCM - Vertically Collimating Mirror

WAXS - Wide Angle X-ray Scattering

XAFS – X-ray Absorption Fluorescence Spectroscopy

XRT – X-ray Ray Tracing

1. Overview

The Dutch Research Council (NWO) has invested in access to synchrotron radiation (SR) for over 35 years. First access to SR for Dutch users was achieved by funding of a SAXS beamline at the Synchrotron Radiation Source (SRS) (Daresbury, UK) which also gave Dutch users access to other SRS beamlines. As a result there is a strong Dutch user community in x-ray spectroscopy, interface diffraction and time-resolved SAXS. The closure of the SRS required access to another SR source for which the ESRF was chosen and through collaboration with Flemish partners the DUBBLE project, was established. The DUBBLE BM26B beamline has been in operation for more than 15 years. In this time it has produced data for close to 700 manuscripts and that number is growing at a rate of about 60 manuscripts/year with an average journal impact factor of around 6. The main technique is time resolved small/wide angle scattering using a wide variety of sample environments. Over the years, the infrastructure has evolved in such a way that complicated sample environments and auxiliary non-x-ray based techniques can be applied. An option for micro-radian diffraction has been developed which effectively is an example of an ultra small angle scattering technique.

After the ESRF machine upgrade, planned for 2019/20, it is no longer possible to accommodate two beamlines on a single port and either BM26A or BM26B (the SAXS) beamline must be relocated to a new bending magnet port. There are two reasons to keep BM26B at its current port. First, the SAXS beamline has a dedicated experiments hutch that is bespoke and large enough to accommodate a range of camera lengths. Second, the optical components for the SAXS beamline are positioned closer to the position of the smaller x-ray fan produced by the new source.

This document captures the key beamline parameters for a proposed state-of-the-art x-ray SAXS/WAXS beamline located at the BM26 bending magnet port of the upgraded ESRF synchrotron radiation source. We then continue with a close look into the source options provided by the ESRF for CRGs with the aim to select the best one for SAXS/WAXS use. After the choice of source we proceed by considering each beamline component in sequence. A detailed beamline layout is presented in which key design decisions are described and contrasted with alternative approaches. Where appropriate, we have included potential future upgrades that would provide new capabilities. For example, the introduction of a transparent monochromator would allow users to make use of the existing BM26A experiments hutch and associated beamline vacuum pipes and pumps. The details of the optics of the third beamline is not further specified at this moment in time, several options are open to an extended user community which range from high-resolution tomography to coherent beam diffraction imaging.

To support the design choices we have made extensive use of ray trace calculations (XRT v1.1.0 & SRW3.92) [1].

2. Scientific Case

The DUBBLE project consists of two beamlines with an infrastructure specifically developed for the Dutch-Flemish (DF) user community. From these developments the ESRF user community also has benefitted throughout the years as evidenced by the oversubscription factors in the publicly available beam time. Lacking a national SR source, the amount of SAXS/WAXS beam time available for the DF user community via the ESRF public beamlines, and other European sources, is wholly insufficient hence the proposed requirement for a dedicated beamline. In view of the oversubscription of the 30% public beam time it is evident that the DUBBLE SAXS/WAXS facility caters for a substantial demand from the larger ESRF user community as well.

The continued and increasing amount of research, within the DF science remit, in nanotechnology, self assembly, novel materials, *etc.* requires a continued access to characterization methods that provide information on the Angstrom to micron length scale in a time-resolved fashion such as provided by combined SAXS/WAXS instrument. It is not foreseen that this demand will diminish but instead one can predict that increased interest in, for instance, areas like food technology in combination with a higher demand in grazing incidence SAXS will only increase the demand for access to X-ray scattering.
Most of the experiments carried out on the beamline are time-resolved where the time-resolution is set by the evolution of sample structure and not necessarily by the speed which is allowed by the beamline/detector combination. The increase in flux and a smaller focal spot will improve the time and spatial resolution even further, ready for a key role in delivering on advanced materials characterisation tasks.

Over the years the infrastructure has evolved in such a way that complicated sample environments and auxiliary non-X-ray based techniques can be applied. Large-scale installations can be accommodated - like for instance vertical detector geometry measurements, experiments using capacitor banks to drive 30 Tesla pulsed magnets, complete vacuum systems for in situ nano particle growth, *etc*. More common are the fibre spinning/film blowing polymer-processing installations, which are also rather large scale. Smaller scale equipment like: flash differential scanning calorimetry, adapted rheometers, shear cells, supercritical CO_2 processing, *etc*. has appeared on the beamline throughout the years.

Small angle x-ray scattering is applied to systems that are either difficult or impossible to crystallize, are complex or composite systems or materials with varying degrees of self-organisation. The wide range of sample types suitable for study using small angle scattering makes this technique suitable to many applications that range from protein shape analyses in solution through to phase behaviour, catalysis, advanced materials development and engineering. Extensions of the traditional small angle setup to ultra small angles on the one hand and wide angle scattering on the other allow studies over a large range of length scales. In figure 1 an overview is presented that captures spatial resolution and sample volume for various X-ray techniques and non x-ray methods of microscopy such as scanning tunnelling, atomic force and electron microscopy.

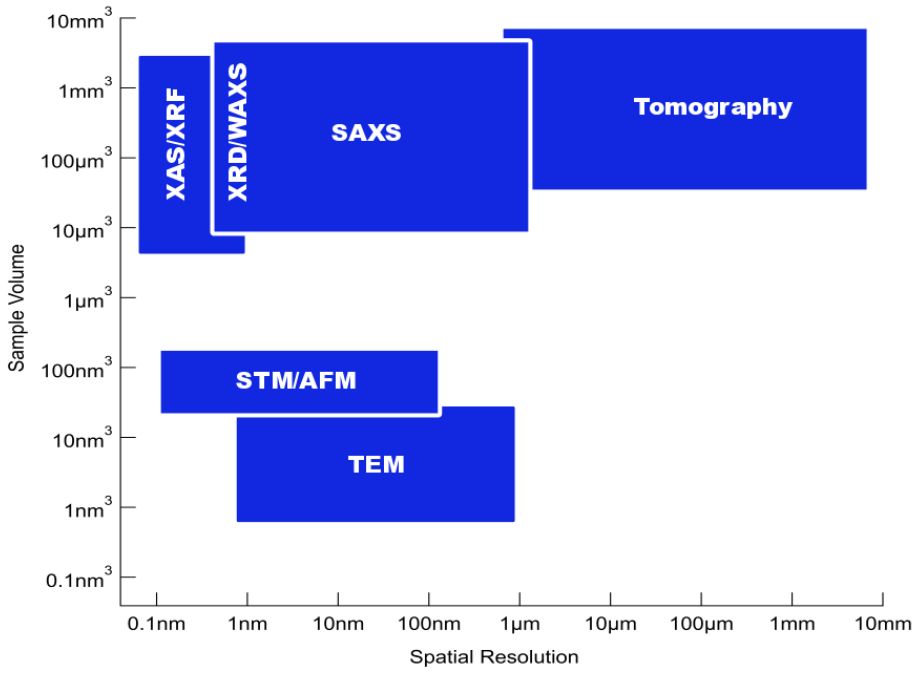

Figure 1: Sample volume versus spatial resolution achievable for various techniques. STM/AFM and TEM are microscopy techniques that do not use x-rays and as such are complementary to x-ray techniques such as listed. Tomography sample volume is truncated and extends upwards.

With the ESRF machine upgrade and improved optics, the current SAXS/WAXS capability will be extended on several fronts; reduction of sample volume and increased spatial resolution, extension of SAXS spatial resolution to create an overlap with (SAXS) tomography and decrease in exposure time.

Traditionally, samples are studied under transmission conditions making use of the high penetration depth of x-rays. More recently, grazing incidence and/or grazing exit geometries have been applied successfully allowing the beam to probe only thin functional layers and reducing background and bulk scatter contributions. To conduct such grazing incidence measurements more regularly, the available interface diffractometer should be placed at or near the sample position. This system provides an excellent wide-angle scattering capability for both vertical and horizontal scattering vectors in addition to a very stable sample mount for loads up to several 100's kg.

The departure of its sister beamline, BM26A, to its own bending magnet port allows the introduction of a third facility for our users which will be housed in the former spectroscopy experiments hutch (BM26A) with a relatively small level of investment albeit with restrictions in terms of available space. Due to the geometry this side station will have a limited energy range that can't be scanned quickly rendering this side branch most useful for fixed energy operation.

3. Key design choices

The beamline is to provide a versatile and highly productive facility for X-ray scattering for a wide range of scientific disciplines:

- Polymer processing
- Colloidal suspensions
- Nanomaterials and condensed matter research
- Functional materials and systems
- Life science and biology

To achieve the above goals and to attract (and continue to do so) the best science the proposed beamline must feature:

- Wide range of momentum transfer by combining both WAXS and SAXS ranges
- Low parasitic scattering
- Flexible sample environment
- High time resolution
- Option for ultra-low angle scattering with crystal collimators

Key design decisions are indicated by red arrows (➔), sections that require further action are marked with ☒. Optional items that enhance and extend the use of the beamline are highlighted by ⓘ. The ❖ - symbol is used to indicate some useful numerical results.

Key information regarding the ESRF machine upgrade and the new insertion device specifications were taken from the briefing document by J. Chavanne [2].

3.1 Energy range

➔ 5 - 25 keV

Ideally the energy range of the beamline would be as large as possible allowing users maximum flexibility in selecting X-ray energy. This flexibility allows doing anomalous scattering experiments but also providing a means to select a large coherent fraction of the beam. Realistically, however, this photon energy range is limited by source properties, method of monochromatisation, reflectivity of optical elements, absorption by vacuum windows, *etc*. On the side of the energy spectrum with lower energies, one will have access to a very large coherent fraction that will allow users to conduct coherent X-ray imaging experiments whereas at the high-end deeper penetrating beams are available to study interfaces. The ability to vary the energy selected smoothly allows quick changes but also provide a means to conduct anomalous scattering experiments with enhanced contrast for specific elements.

To cover the full range of energies various combinations of monochromator crystal type, mirror coating and mirror angle are required. In order to remove third harmonic contamination operation of the beamline we can identify three energy ranges that can be accessed with the same combination of optical components: 5-15 keV and > 15 keV. The proposed design is optimised so that switching between the various configurations is quick and automated.

3.2 Radiation source

➔ *It is proposed to use the SBM as the source for the SAXS/WAXS beamline.*

The ESRF EBS upgrade has a considerable effect on the operation of CRG beamlines. The new low-emittance lattice proposed is using multiple bending magnets with a reduced magnetic field as opposed

to the magnets in the old lattice. To overcome this lack of a suitable source with similar critical energy for future CRGs, the ESRF has proposed three schemes (table 1) that use dedicated insertion devices located at a position close to the existing bending magnet.

Insertion Device	Number of magnet poles	Horizontal Divergence (mrad)	Magnetic Field (T)
Short Bending Magnet (SBM)	1	2	0.856
Two pole Wiggler (2PW)	2	1.7	0.856/0.856
Three pole Wiggler (3PW)	3	1.6	0.5/0.856

Table 1: Overview of insertion devices available to CRGs at the ESRF.

Of the three schemes only one (SBM) uses a canted magnet arrangement to avoid interference of radiation from neighbouring bending magnets. For SAXS experiments in particular it is important to provide a beam free of parasitical scattering with radiation emanating from a single point source. The highest flux across the energy range is provided by the 2PW which will be double that of the SBM whereas the 3PW output will lie between these two due to the fact that two of its poles are only 0.5 T in strength.

The choice of the SBM as the new source will not provide a larger integrated flux at the sample position compared to the current situation at BM26B because the magnetic field strength is identical to that of the existing dipole magnet. For experiments that require a significant flux increase it is proposed to use a multi-layer monochromator with a larger bandwidth. Such devices have been used elsewhere with good results and provide up to *two orders* of magnitude larger photon flux as opposed to a factor of two for the 2PW option. Combining the existing monochromator vessels from BM26A&B an inline or series setup would allow a quick changeover between the two types of monochromators. This keeps options open to perform anomalous small angle scattering or x-ray spectroscopy experiments.

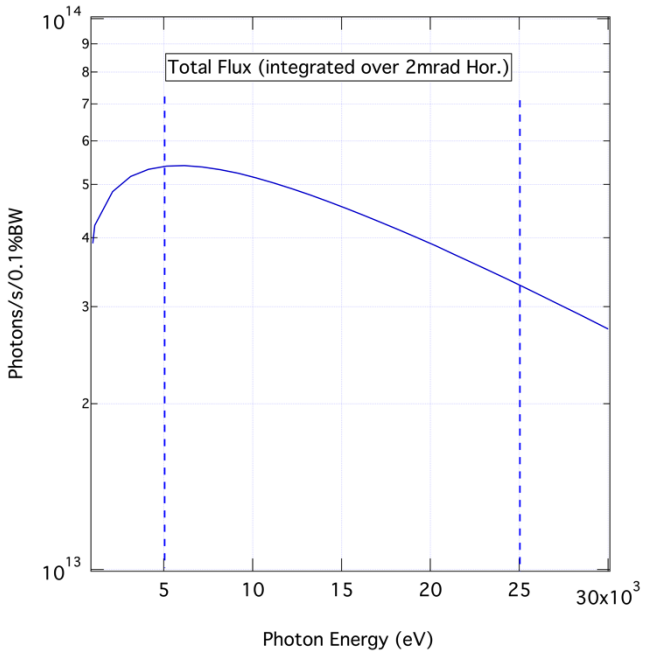

Figure 2: Integrated flux for the Short Bend Magnet source.

The total flux curve has been calculated with the usual assumption of a 0.1% Band Width (BW) which is approx. one order of magnitude larger than that of a Si(111) monochromator. Therefore, expected flux

at the sample will be below 10^{13} photons/s. In practical cases - where a smaller acceptance angle is used in combination with two (non-ideal) mirrors - the expected flux is in the range 10^{11} - 10^{12} photons/s.

The bandwidth for a multilayer monochromator can reach 2% or more and thus boosting the available monochromatic flux significantly if and when required.

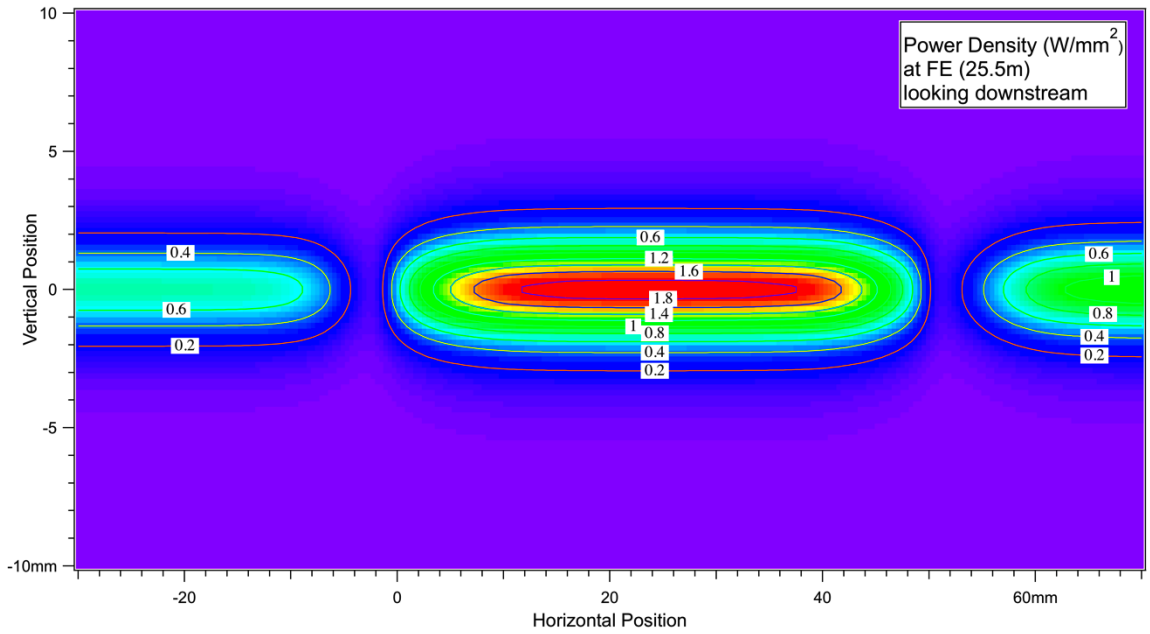

Figure 3: Power density at the exit of the frontend (FE). Either side of the SBM radiation fan (2 mrad), the contributions from the neighbouring combined dipole/quadrupole magnets (DQ1D & DQ2C) can be seen. The storage ring current was taken to be 200 mA.

Compared to the existing source, the upgraded machine offers a significant reduction in electron beam cross-section and horizontal emittance. In table 2, we compare the changes between the current source and that of the upgraded one. Looking at the so called beta functions which describe the horizontal and vertical size of the electron beam it seems that in the new lattice the electron beam cross section at the location for CRG ports is small compared to other positions around the lattice. Therefore one can expect significant gains in brilliance of the upgraded facility, which will particularly benefit experiments that require small and bright beam spots for sample probing provided that suitable focusing optics is used.

The coherent fraction of the beam will be larger; an interesting feature which we will investigate later in this report.

	Current High/Low Beta	After Upgrade
Hor. Emittance (ε_x) [pmrad]	4000	130
Vert. Emittance (ε_y) [pmrad]	5	5
Hor. RMS beam size [µm]	98/132	23
Vert. RMS beam size [µm]	11/13	3.6

Table 2: Electron beam parameters before and after upgrade (source: ESRF)

- *This choice is motivated by the fact that of the three options only the SBM source provides a single source clear from overlapping parasitic sources with a well understood photon beam profile.*

As mentioned earlier, there will be no improvement in total available flux compared with the existing source but with the significant increase in source brilliance, the new source will provide a large increase in flux density at the sample. Thus providing much faster measurements on smaller sample volumes.

3.3 Momentum transfer (Q) range

For SAXS experiments the angular resolution must be significantly better than for a generic x-ray diffraction experiment. A range of merely 6° angular range corresponds to two decades in real space. With the decrease in source size one can expect the angular resolution to improve With a SAXS range of camera lengths ranging from a few centimetres to 11 meters, the Q-range provided to the user runs to 0.0175 nm^{-1} corresponding to a real space range from to 500 nm. This real space measurement range is complemented by a WAXS diffraction angle range op to 40°.

An option to push real space resolution well into the micrometer range is provided by an optional Bonse-Hart setup which is currently under development in collaboration with others.

3.4 Coherence

The reduction in the (horizontal) source size increases the transversal coherence length of the source. The coherent fraction is usually found using (assuming a Gaussian beam shape):

$$\frac{I_{coh}}{I} = \frac{\lambda^2}{(4\pi)^2 \varepsilon_x \varepsilon_z}$$

where λ is the wavelength of the radiation, and ε_x, ε_y the source emittance in the horizontal and vertical directions. For the 2PW wiggler, we get 0.6 for λ = 2.5Å wavelength and 0.09 for λ = 1Å.

In order to arrive at a practical estimate of fully coherent flux we use the generic point source expression for the transverse coherence length using slits:

$$\ell_{c_{x,z}} = \frac{\lambda D}{2\sigma_{x,z}}$$

At a distance (D) of 50 m from the source we arrive at a transversal coherence length of 110 x 625 μm^2 (*hxv*). Within this cross section the beam is fully coherent for a monochromatic beam with an energy of 12.4 keV. At 5 keV the transversal coherence length increases to 0.28 x 1.6 mm^2 (*hxv*). Often a less restrictive condition of partial coherence is sufficient allowing a larger beam to be used. In photon correlation spectroscopy slit width values of twice the above coherence length are used for obtaining the best signal-to-noise values. Using a secondary set of slits a range of coherence lengths can be obtained [3].

- *Using ray tracing we find that the fully coherent flux at 50 m distance from the source 10^8 photons/s at 7 keV.*

The expected coherent fluxes are sufficiently high to consider static (Bio-) CXDI (Coherent X-ray Diffraction Imaging on biologically interesting samples) experiments at 5 keV especially considering that one can use focusing optics after the coherent fraction selecting slits allowing the coherent flux to be

incident into a sub-micrometre scale volume. For comparison: a single XFEL pulse - which is almost fully coherent - has 10^9 photons. For comparison: ID10 dedicated ESRF insertion device beamline has a coherent flux of about 10^{10} ph/s at 7 keV.

3.5 Beamline stability criteria

Considering the beamline as a microscope with a primary figure of merit determined by spatial resolution one can readily derive some key stability criteria assuming the simplest of optics consisting of a single focusing element. Using the full available space offered to CRG teams with the experiments hutch at about 50 m and the sample 0.05 m from the focusing optics one has a demagnification factor of 10^{-3}. With a source size of approx. 25x4 μm^2 (*hxv*) one can thus expect a focal spot size of 25x4 nm^2 assuming ideal focusing conditions. More realistic focal spot size taking account of realistic mirror optics would be *50x20 nm^2*.

Considering the x-ray spot size of 50 nm and an acceptable beam drift of 10% of its size would result in a 5 nm translation. This should be respected over the duration of the scan or experiment of, say, 60 minutes. The angular tolerance is taken to be a 10% beam spot shift over the focal length of 0.05 m, which results *in an angular stability of 100 nrad again over a typical time of 1 hour*.

The above figures require careful design and above all avoiding relative temperature changes between components. Sample and microfocusing optics mounting should use a common rigid structure, a departure from existing approaches to support key focusing elements.

4. General beamline layout

An overview of the proposed beamline with its main components is shown in figure 4. For clarity filters, beam shutters, absorbers, beam diagnostics and potential upgrades are not shown. The proposed design features ease of operation whilst making full advantage of the expected large increase of brilliance without compromising the high angular resolution. The design is inspired by the existing hutch infrastructure, which consists of a large optics hutch and two experiments hutches. With the transfer of the x-ray spectroscopy beamline (BM26A), the hutch located at about 40 m from the source becomes vacant. With a Laue setup it is possible to channel monochromatic radiation into this hutch to establish a third technique: multi mode x-ray imaging.

With a relatively simple optical scheme it is possible to create finely focused beams or expanded beams for high-resolution imaging of large (0.1 m) objects. The focusing mirror for this branch is shown in the reflecting up geometry for practical applications one would reflect the beam downwards similarly as it is done in the existing setup.

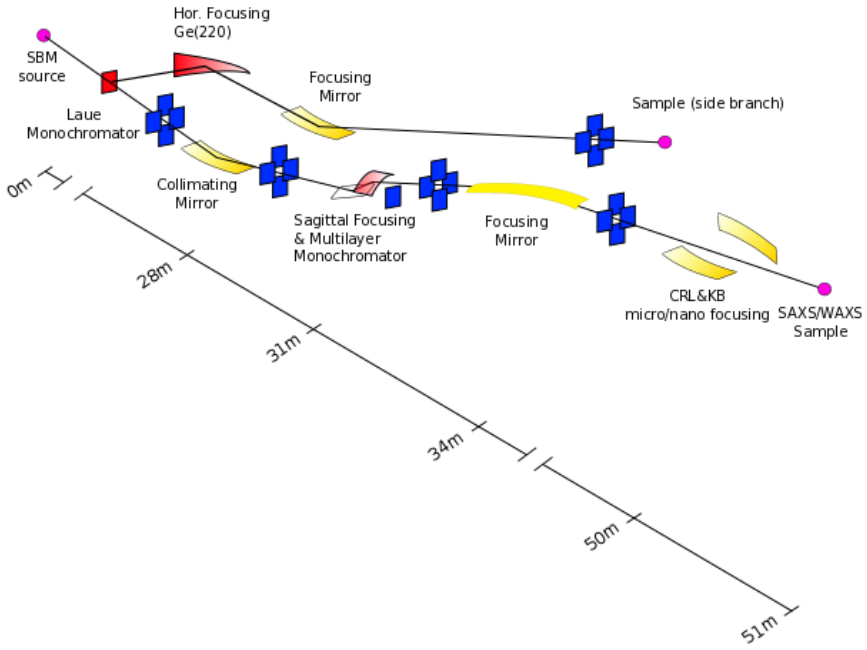

Figure 4: Proposed SAXS/WAXS beamline layout showing side branch station, which receives radiation from a Diamond (111) Laue monochromator in transmission mode (not to scale). The white beam exits the front end at a distance of 25.5m from the source.

The configuration shown in figure 4 has an up-up-down-down deflection geometry, which provides an effective way of blocking Bremsstrahlung using a beam stop down stream of the first monochromator crystal. An alternative arrangement would result in height changes of the various components and sample compared to the existing situation. A detailed description of each beamline component is given in the following sections. The sample position is variable to allow for flexibility in sample environments and additional equipment. Horizontal focusing for the SAXS/WAXS station is accomplished with a sagittal focusing monochromator. The sample will be located at 51 m from the source, which corresponds to a 1.6:1 demagnification of the source. Within the existing hutch constraints the maximal sample to detector distance will be 11 m.

4.1 Front end

A 4x1 mrad^2 aperture is used close to the source to protect vacuum chambers. Currently the ESRF CRG front end uses a 0.5 mm thick Be window placed close to the tunnel wall (25 m from the source) which seals the machine vacuum from that of the CRG beamline. This relatively thick window introduces a cut-off at about 5 keV; figure 5 shows ray trace results for the footprint of the beam and energy spectrum that is absorbed by the Be window. Reducing the window absorption would benefit experiments conducted at low energies such as those exploiting the coherent fraction, which is highest at low photon energies.

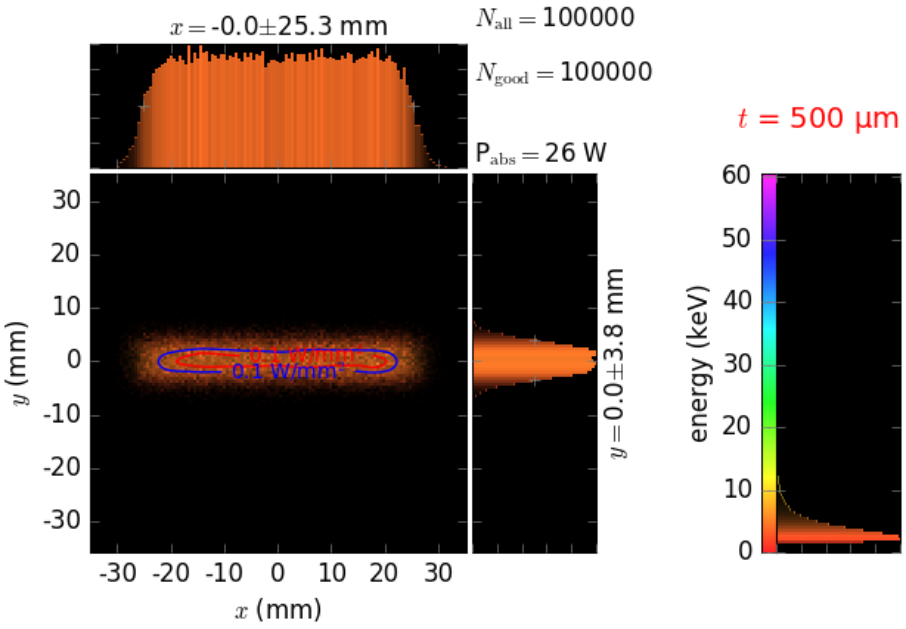

Figure 5: Ray trace results showing beam footprint on frontend Be window with a thickness of 0.5mm. The window absorbs 26W at 200 mA ring current. On the left the part of the energy spectrum is shown that is absorbed. N_{all} refers to the number of rays that were used in the calculations.

Traditionally the ESRF equips their standard front-ends with X-ray beam monitors that intercept the edges of the white beam. Such monitor reading would be helpful for the beam line and hopefully their signals will be made available to the CRGs.

☒ *Efforts should be made to either remove this window completely or to decrease its thickness to 0.2 mm so that approx. 85% transmission is achieved for 5 keV photons.*

4.2 Collimating Mirror

A collimating mirror will be introduced as the first optical element that is exposed to the white beam. This vertically collimating mirror (VCM) is capable of collecting the full white beam cone as transmitted through the front-end mask. (The ESRF has opted to insert a 4x1 mrad^2 (*hxv*) aperture that is larger than the insertion device divergence but nevertheless useful to remove surrounding dipole contributions). The VCM has two functions:

- collimating the incident beam to provide a better energy resolution, and
- removing high-energy photons which would be transmitted as higher harmonics and spoil measurements. At the same time this low-pass filter reduces the heat load on the monochromator significantly.

For a Si(111) monochromator crystals, the strongest harmonics are the third order ones. Therefore starting at 5 keV photon energy, the cut-off energy is set at 14 keV.

Traditionally, a 1.2 m long, flat mirror is used which is polished to the highest standards and bent into a cylindrical shape by mechanical means creating only a vertical collimation of the beam. In order to create the required energy cut-offs for the above ranges one would need two different coatings and two different angles of incidence as shown in figure 6.

Besides Si either Rh or Pt coatings would be required for the higher range of energies (above 25 keV). Below 25 keV it only makes sense to use Pt coatings if one would like to collect more than about 0.1 mrad of vertical divergence. Note that the calculation represents the reflectivity for one mirror only.

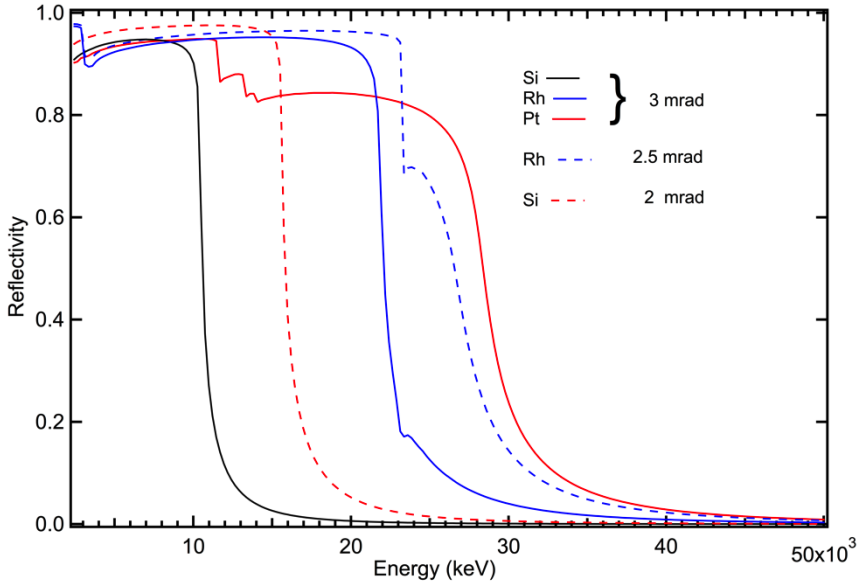

Figure 6: Mirror coating and angle of incidence for SAXS/WAXS optimised for the photon energy range of 5-25 keV. Note that the calculation concerns the reflectivity of a single mirror. The beamline will have two such mirrors in a non-dispersive arrangement (+-).

Capturing the full 2 mrad horizontal divergence with the VCM located at 28 m from the source requires strips with a width of approx. 50 mm leaving no room to add a third strip. Preference is for two strips: Si and Rh thus avoiding Pt edges around 12 keV. Alternative would be to work with three strips of about 30 mm width each collecting no more than 1 mrad. This reduction is not a serious issue because the monochromator will be limited to capture up to 40 mm of beam width.

In order to cover the full energy range one can readily distinguish three sub-ranges for which a different mirror coating or angle of incidence must be chosen (see table 3). Although it is possible to choose different angles of incidence for the two mirrors, one would try and avoid this so that the beam near the sample is travelling in a horizontal plane.

Photon Energy	VCM coating	Angle of incidence
5 – 14 keV	Si	2 mrad
14 – 25 keV	Rh/Pt	2.5/3 mrad

Table 3: Mirror coating and angle of incidence for creating energy cut-offs.

The use of a doubly curved mirror surface would be too restrictive and compromise the capability to tune this mirror to different cut-off energies. The use of mirrors to focus the beam above energies of about 35 keV becomes problematic due to the very shallow angles.

The meridional radius of curvature is given by:

$$R_m = 2p \sin^{-1} \alpha,$$

where *p* is the source to mirror distance and α the angle of incidence of the beam. For practical situations this results in a radius of curvature that is rather large (>10 km) and a good gravity compensated bender will be required.

☒ *The power density levels on the VCM are relatively low due to the small angle of incidence. With a total absorbed power of less than 100 W an arrangement such as currently used at BM26A consisting of side cooling using liquid metal filled grooves is sufficient.*

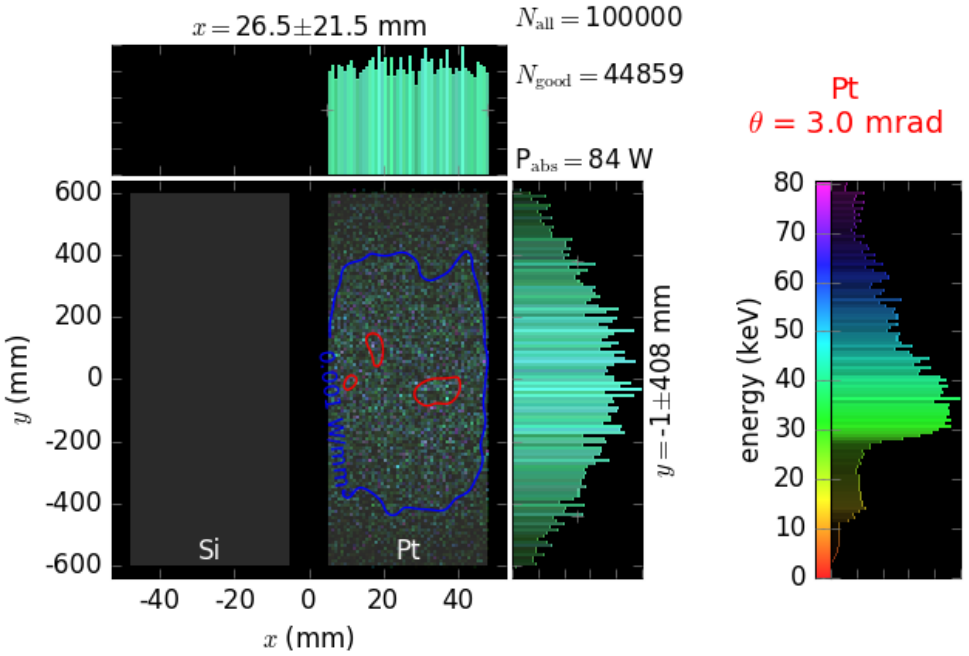

Figure 7: Heat loading of VCM for a Pt coating at an angle of incidence of 3 mrad. Note that a two stripe coating was used each with a width of approx. 40 mm capable of capturing 1.4 mrad of the 2 mrad wide fan of dipole radiation. The absorbed photon energies are shown on the right demonstrating that photon energies above 30 keV are removed from the reflected beam.

4.3 Sagittal Focusing Monochromator

➔ *It is proposed to use a Double Crystal Monochromator (DCM) with sagittal focusing second crystal.*

The use of a sagittal focusing monochromator provides an elegant way of creating a monochromatic beam, with the ability to dynamically focus the beam horizontally at an arbitrary point downstream of the monochromator. This is of importance not only for the case in which the sample location varies but also for the case in which the beam is focused on the detector or when additional downstream optics is used. Fixed focus optics such as a toroidal mirror would be less suitable.

Unfortunately, the use of bend crystal optics has well documented issues that are related to the fact that it is very difficult to create a perfect cylinder shape by bending a thin crystal of sufficient width to capture a significant amount of the 2 mrad radiation fan. Traditionally reinforcing ribs are used to avoid the anticlastic distortions. With the large reduction in source size, however, the use of a fully ribbed second crystal becomes unacceptable because the rib width dictates the minimum achievable horizontal beam size due to the fact the crystal stays flat underneath a rib. In order to address this issue a modified

crystal is proposed (see figure 8). Detailed finite element studies show that this approach is feasible. The use of a 120 mm long (in the direction of the beam) crystal with only two thin ribs results in a large, usable cylindrically curved area. The ratio of width and length of the crystal has been optimised. Two thicker sections are clamped in a precision dual moment bender mechanism that keeps the crystal surface at a constant height. Good solutions are available commercially, which can be adapted for the proposed crystal size. Just like the upgrade of the BM26A monochromator it is possible to upgrade only the crystal cages of the existing DCM whilst keeping the existing vacuum chamber and Bragg angle axis.

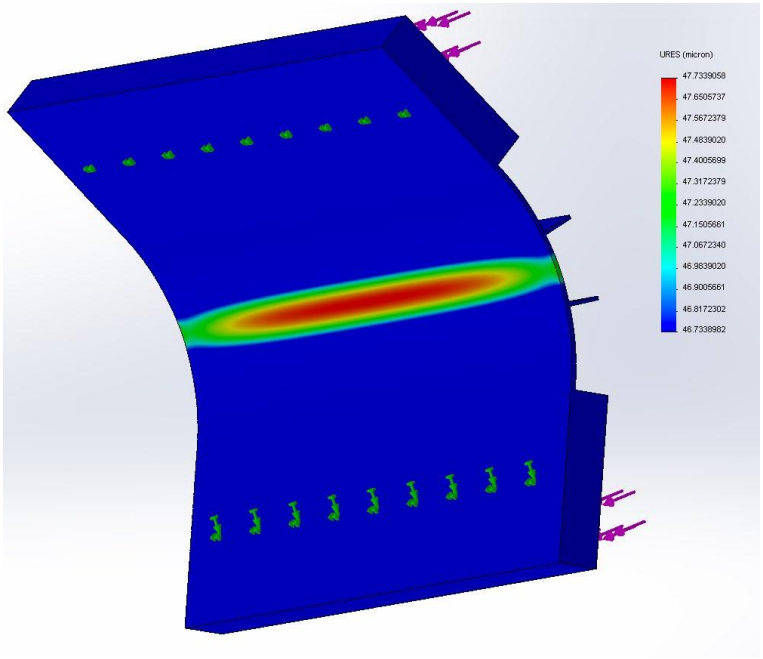

Figure 8: Sagittal focusing second crystal proposed. The cylindrically bent crystal only deviates from the ideal shape near the two sides as evident from FE calculations. A symmetrically bending moment is applied to the thicker parts of the crystal (indicated by green and purple arrows).

To capture the full 2 mrad beam at the position of the DCM, the beam width at the monochromator is approx. 60mm. The above approach with only two ribs works for a maximal 'rib-less' width of 15 mm or 0.5 mrad. In principle the crystal can accept the full source divergence with the aim of increasing the flux at the sample to the maximum available albeit at the cost of a larger spot size at the sample. For achieving the smallest measurable angle, as we shall discuss later on, one should limit the width of the horizontal fan of radiation collected with practical values no larger than about 20-30 mm. Restricting the central area is, therefore, not a severe restriction.

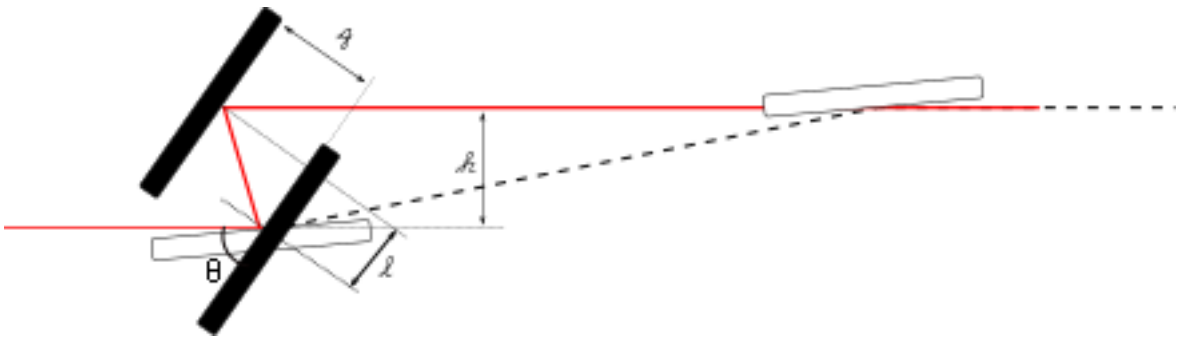

Figure 9: DCM setup geometry for low (filled) and high (open) energy setting.

In figure 9, we have superimposed the location of the monochromator crystals for the lowest (black filled rectangles) and highest energy (white filled rectangles) setting for the proposed energy range of 2.4 - 30 keV. From this diagram it is clear that (apart from the Bragg angle rotation) the crystal gap and crystal translation settings are energy dependent if one wants to keep the exiting beam at the same height. The two relationships for a DCM with a fixed exit height (h) are:

$$\ell = \frac{\hbar}{2\sin\theta}$$

$$g = \frac{\hbar}{2\cos\theta}$$

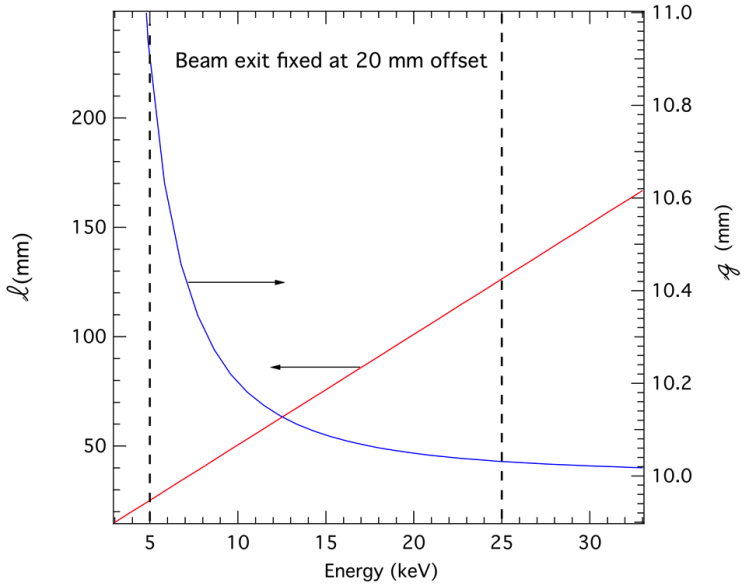

Figure 10: Monochromator translations for second crystal required for fixed exit operation

For a fixed exit operation mode the gap (g) between the two crystals must be adjusted, albeit over a relatively small change. With a beam offset (h) of 20mm and crystal length of at least 120 mm the full range of 5 – 25 keV is just about covered (see figure 10). Thus as the energy is changed within the above energy range, the beam 'walks' along the second crystal. To avoid loss of monochromatic beam or the use of a larger crystal, a translation stage is required to move the second crystal to the calculated position.

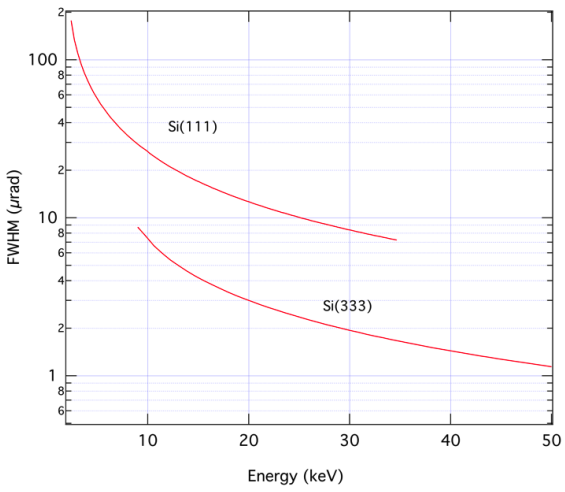

Figure 11: Angular Darwin width of the Si(111) reflection and its third harmonic.

The energy resolution can be found readily using the relationship:

$$\frac{\Delta E}{E} = \frac{\zeta}{\tan\theta}$$

A Si(111) monochromator has an energy resolution of $1.3\text{x}10^{-4}$. For its third harmonic, the Si(333) reflection, one can also expect an appreciable intensity. For Si(333) the energy resolution is $0.3\text{x}10^{-4}$ (see figure 11). The tradeoff for the higher energy resolution is a lower flux and the relative intensities of the two differentreflections are shown in table 4.

Crystal plane	Intensity	Energy Resolution (ΔE/E)
Si(111)	45.85	$1.26\text{x}10^{-4}$
Si(333)	15.88	$2.90\text{x}10^{-5}$

Table 4: Monochromator intensity and energy resolution comparison

4.3.1 Heat load

In the worst case scenario (large Bragg angle corresponding to 5 keV, no collimating mirror) the first crystal is exposed to the white beam with a peak power density of 0.5 W/mm^2 with a total loading approx. 200 W (see figure 12). A more realistic calculation with collimating mirror shows a loading of about 100 W with a power density of 0.38 W/mm^2 (see section 5.1). We have assumed a frontend vacuum Be window with a thickness of 0.2 mm. Reducing the thickness or removal of the Be window altogether has advantages for measurements with low energies but results in a marginally larger heat load of the monochromator. For intermediate and high photon energies a (re-)movable filter can be used to absorb the lowest photon energies and thus reducing the monochromator heat load (see section 5.1).

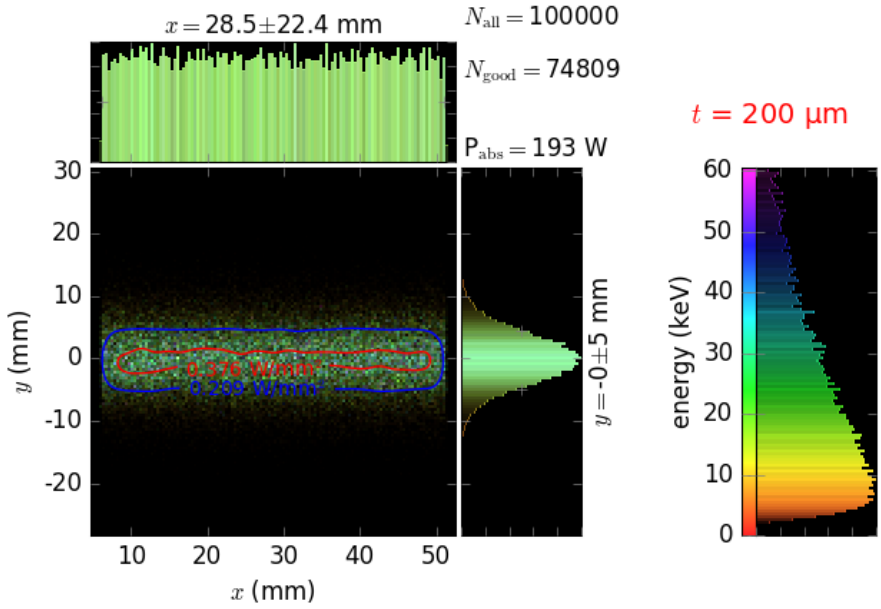

Figure 12: First monochromator crystal heat load calculated by ray trace calculations performed at a DCM setting of 5 keV using the full available beam without collimating mirror and a single Be window of 0.2 mm thickness. The incident spectrum

is shown on the right. The total power absorbed by the crystal is shown as P_{abs}. The contour levels are at 50% (blue line) and 90% (red line).

Given the fact that the angular Darwin width (or acceptance angle) of the Silicon crystals is of the order of micro-radians, we have to keep thermally induced distortions to a minimum. Requirements for cooling of the optical components that are exposed to the white beam are discussed in a separate section later in this document.

4.4 Vertically Focusing Mirror

➔ *A vertically focusing mirror (VFM) is chosen which is bent to provide a focal spot at the sample position.*

The collimated, horizontally focused and monochromatic beam emanating from the monochromator is to be focused in the vertical direction and a focusing mirror is required. Traditionally large single crystal silicon mirror blanks are used that are bend mechanically into the required shape. Recent progress with piezo electric single mirrors has resulted in very low slope error mirrors that seem ideal for focusing the monochromatic beam (http://seso.com/en/news/bimorph-full-potential/).

Typically the meridional curvature is large as described by:

$$R_m = 2\,q\,\sin^{-1}\alpha$$

Here q is the mirror to focal spot distance. For the meridional radius of curvature we get a value of R_m = 14 km with a collimating mirror or 9.4 km without one.

By horizontal movement, one of the two surfaces can be selected giving the user a wide choice in cut-off energy and focusing conditions. In order to capture most of the vertical extend of the beam a mirror of about 1.2 m long would be used with a width of 100 mm. Such a mirror would be identical in size as the current flat mirror allowing its vacuum vessel and translation stages to be reused.

A single flat mirror fixed at a variable incidence angle will cover a wide range of energies up to about 25 keV (see table 5 and figure 6).

Photon Energy	VFM coating	VCM coating	Angle (mrad)
5 – 14 keV	Si	Si	2
10 – 25 keV	Rh	Rh	3

Table 5: Mirror coating combinations and mirror incidence angles for two energy ranges required to avoid third harmonic contamination. Pt coating would result in absorption 'features' near 11 keV, since beamline is not required to provide eneriges above 25 keV a Pt coating isn't needed.

The combination of horizontal focusing with the sagittal focusing DCM en vertical focusing with a mirror gives full control over focal spot size and location of the focus allowing geometries in which the beam is focused on the sample, detector or even the use of an unfocused beam.

4.5 Ray tracing

Because of the significant source size reduction the quality of the mirrors used becomes very important. Ray trace calculations were performed with mirrors of varying slope error to avoid introducing significant losses in source brilliance. In order to perform realistic simulations of beamline performance we have contrasted perfect mirrors with real mirrors that have roughness and slope errors.

The slits were set such that horizontally 1 mrad was accepted whereas in the vertical direction the number was 0.1 mrad. *To focus the SBM source without significant distortions mirror slope errors must be smaller than the angular size of the source or 4 µm/34 m= 0.1 µrad.* Unfortunately this figure is difficult to achieve for mirror of sufficient length.

- For mirrors with RMS slope errors of 0.65 µrad which corresponds to a finish which is affordable, ray trace calculations result in a 25x90 (*hxv*) µm^2 FWHM spot size (see figure 13). This calculation was performed for an energy of 10 keV. This compares to a focal spot size of 300x300 µm^2 in the current situation. With the quick pace in polishing and metrology a mirror slope errors of 0.3 µrad are available for flat mirrors with which we should achieve a 25x40 (*hxv*) µm^2 FWHM spot size. Thus providing almost two orders of magnitude improvement in photon flux density at the sample.

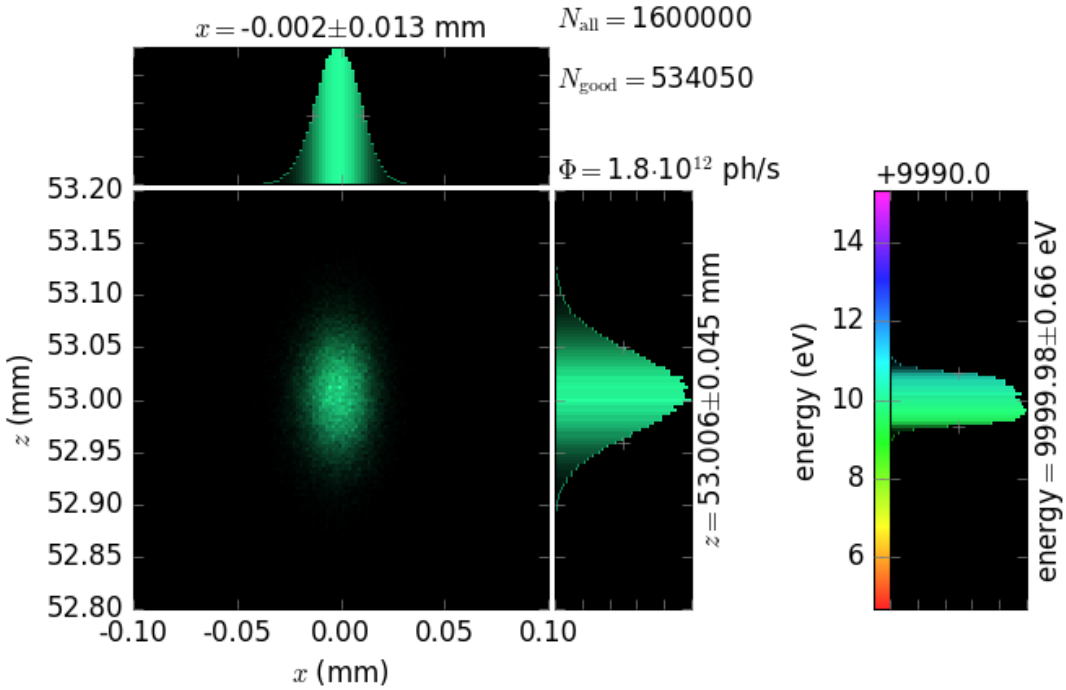

Figure 13: Ray trace calculations for a complete beamline that includes VCM, DCM and VFM. An RMS slope error of 0.65 µrad for both mirrors is used in the calculations. For mirrors without slope errors the vertical focus FWHM will decrease to about 10 micrometre as opposed to 90 micrometres. The sagittal focusing monochromator was assumed to be perfect during the calculations.

4.6 Compound Refractive Lenses

Compound refractive lenses are an interesting option when working at a fixed energy. Apart from the fact that these devices are chromatic, they capture a relative small cone of radiation. Also the devices absorb significant amount of radiation particularly at low photon energies. For the relatively low energy

available at the SAXS/WAXS beamline the best choice would either be CRL lenses made of Beryllium or diamond foil.

Compound refractive lenses are very simple devices to operate but any given setup is optimal for a given photon energy. To overcome this hurdle, the ESRF has developed a system called a transfocator [4] in which a variable number of lenses can be inserted into the beam thus allowing focusing at various x-ray energies. In a typical setup the lenses would be placed about 5m up stream from the focal point.

Using XRT a ray tracing study was performed to use CRL's to create a focal spot at the sample position by placing the CRL's at a distance of 46 m from the source. These refractive x-ray lenses are composed of several double parabolic shaped discs of 1 mm thickness. Calculations were performed for photon energy of 9 keV using only the CRL's to focus the beam; no VCM or VFM was inserted. Slits were used to illuminate the full aperture of the lenses. Two lens materials were investigated: Be and diamond each with the same 1 mm radius of curvature. Due to the fact that only an integer number of lenses can be used the focal point deviates slightly from the exact position as shown for both sets of CRL's in figure 14.

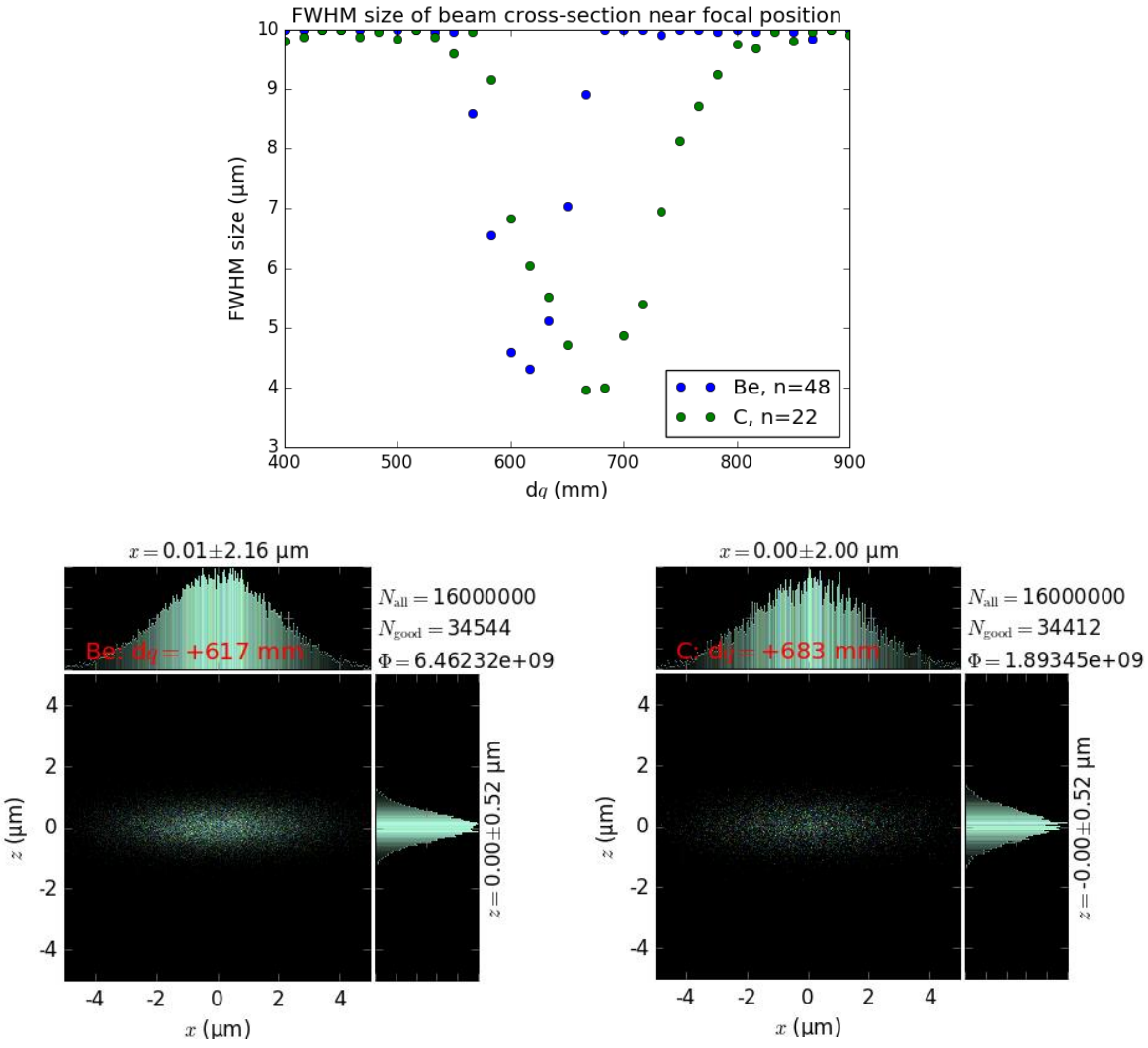

Figure 14: Ray trace results for beam focusing with compound refractive lenses at 9 keV for both Be and diamond lens materials. The x-axis shows the displacement of the best focus from the nominal position of the sample. The number of lenses used is indicated for both materials (top figure). The best focal spot is shown in the bottom two figures (Be: 48 lenses, C: 22 lenses) together with the expected flux.

- *According to the simulations a CRL focusing system will deliver 6x10^9 photons/s with an energy of 9 keV into a 4x1 µm^2 (hxv) focal spot.* This compares to 40x10 µm^2 currently.

4.7 Kirkpatrick-Baez mirror system

The Kirkpatrick-Baez focusing mirrors are non-chromatic and are therefore ideal for energy scanning applications and will operate over the full beamline energy range using two metal coating stripes if necessary. Using a relatively large demagnification (as compared to that of the toroidal mirror) this device allows a significant reduction in focal spot size that is required by experiments that require high spatial resolution spectroscopy measurements. Compound refractive lenses would be an alternative although these focusing elements are chromatic and rather absorbing at lower X-ray energies.

KB mirrors operate with a high demagnification ratio of 100:1 or higher; as a consequence they are placed close to the sample - typically at a distance of 0.2 - 1 m. For the SAXS/WAXS beamline with the sample at approximately 51 m from the source a demagnification ratio of up to 250:1 is possible. DUBBLE has recently taken ownership of a System-I KB mirror system from the ESRF optics group. This focusing optics is able to collect a 0.2x0.5 mm^2 (*hxv*) section of radiation when operating at a 3.5 mrad angle of incidence. The mirrors have a coating of Rh resulting in an energy cut-off of 18 keV.

In order to investigate the best-case focal spot for this KB system it's placed close to the sample at a distance of 250 mm. Ray tracing was performed without further beam optics at an x-ray energy of 10 keV (see figure 15).

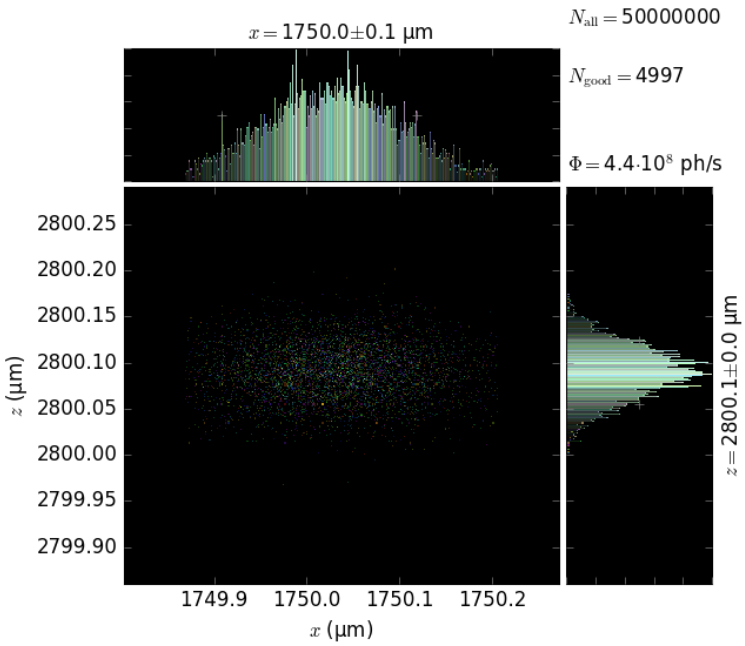

Figure 15: Ray trace results for KB System I mirror system placed close to the sample, which is located at 51 m from source using 10 keV photons. In the calculations the full 0.2x0.5 mm² aperture of the KB system was filled.

Due to the short sample to KB mirror distance, this setup would be placed in the experiments hutch. Because the horizontal size of the beam is larger than the vertical one the horizontal focusing mirror should be the one closest to the sample allowing a higher demagnification than for the vertical direction.

- *According to the simulations a KB focusing system will deliver 4x10^8 photons with an energy of 10 keV into a 0.2x0.1 µm^2 (hxv) focal spot.* This compares to 20x20 *µm^2 with the current setup.*

- *The example KB system used has a rather modest acceptance and KB systems with a larger acceptance could be used to increase the flux albeit at a slightly larger focal spot size but this would need further investigation.*

4.8 Angular resolution

For SAXS experiments the beam defining and guard slits position is important. Figure 16 shows a schematics of the beamline with 'extreme' paths of the X-rays are shown emanating from the source size (d_s) limited or scattered from beam-defining aperture (d_2) or guard aperture (d_3) are shown. The sample position is located just downstream of aperture d_3, Δ is de radius of the beam stop that should be used so that neither the direct beam nor the parasitic scattering from d_2 reaches the detector.

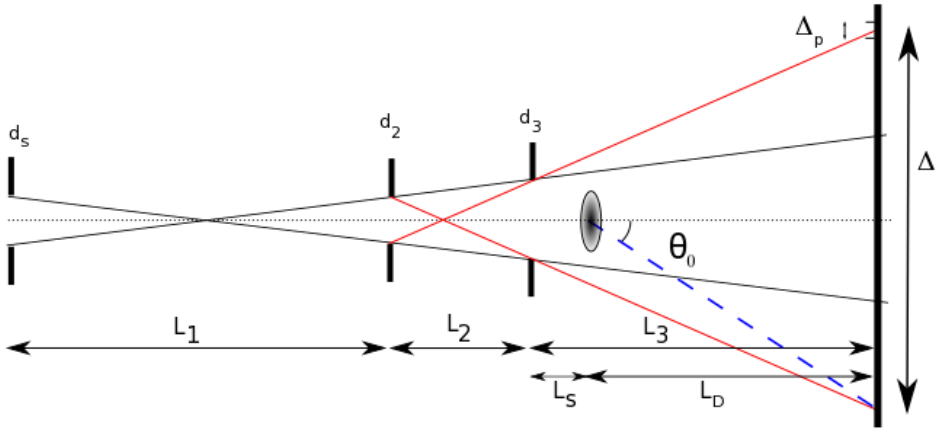

Figure 16: Beam defining slits for an unfocused beamline showing the limiting rays that define the smallest scatter angle θ_0 that can be measured.

The smallest angle that can be measured free of parasitic scattering is θ_0. The slit settings and distances determine the smallest beam stop size for the unfocused beam:

$$\Delta = d_3 + \frac{L_3}{L_2}(d_2 + d_3)$$

The relationship between d_2 and d_3 is given by:

$$d_{3,u} = d_2 + L_2\frac{(d_s + d_2)}{L_1}$$

With these slit settings the smallest angle for the unfocused beamline that can be measured is:

$$\theta_{0,u} = \frac{d_3}{2L_D} + \frac{L_3(d_2 + d_3)}{2L_2L_D} + \frac{\Delta_p}{2L_D}$$

The last term takes into account that the detector has a finite pixel size (Δ_p). With the relationship between the smallest measurable scatter angle and geometry of the beamline defined, the best placement of the various beamline components can be established. Using the existing experiments

hutch layout L_D varies between 0.5 and 10 m. For a fixed total length of the beamline of about 60 m, the following relationship holds: L_1+L_2 = 50 m. L_1 is limited with a minimum of 30 m and a maximum of about 45 m. The setting of d_2 can, in principle, be chosen arbitrarily. However, one should take into account that small settings of d_2 would reduce overall flux at the sample considerably.

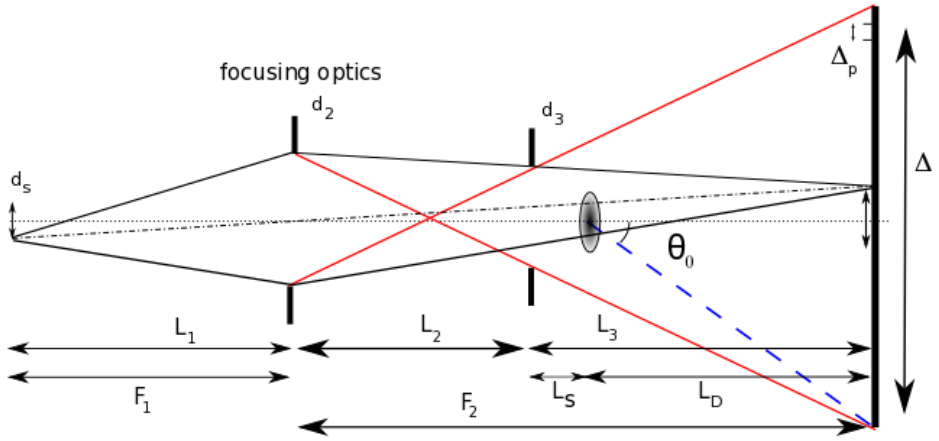

Figure 17: Limiting rays for a focused beamline layout with the focusing optics located at d_2. An image of the source is focused onto the detector which is located on the right hand side.

The smallest scattering angle improves if a focusing setup is available with the focusing element(s) placed at a distance F_1 from the source which has a size of ds as shown in figure 17. The smallest value of θ_0 is achieved by focusing the source onto the detector plane situated at a distance of F_2 from the focusing element(s). At the position of the optics (L_1) the beam size is set by slit d_2 and guard slits d_3 are positioned close to the sample. For this geometry the relationship between d_2 and d_3 is changed to:

$$d_{3,f} = \frac{L_2}{L_1} d_s + \frac{L_3}{L_2 + L_3} d_2$$

Substituting in the above equation for θ_0 gives:

$$\theta_{0,f} = \frac{1}{2L_D}\left[d_s \frac{(L_2 + L_3)}{L_1} + 2d_2 \frac{L_3}{L_2} + \Delta_p \right]$$

Note: in the above derivations we have not considered the fact to a significant part of the radiation is coherent which will influence the results especially for small apertures.

To assess the performance of the beamline for small angle scattering the maximum d-spacing, $d_{max} = \lambda/2sin\theta_0$, is calculated as a function of L_1 using a fixed camera length of 10 m and a wavelength of 1.5 Å, see figure 18.

For the two cases θ_0 behaves differently. Overall the largest values for d_{max} are reached for the focused beamline with the focusing optics as close as possible to the source. For the unfocused beamline the best results are achieved for a value of L_1 close to 30 m from the source, which corresponds to a 1:1 focusing setup, L_2 was fixed at 0.2 m which seems a relastic distance for most sample environments.

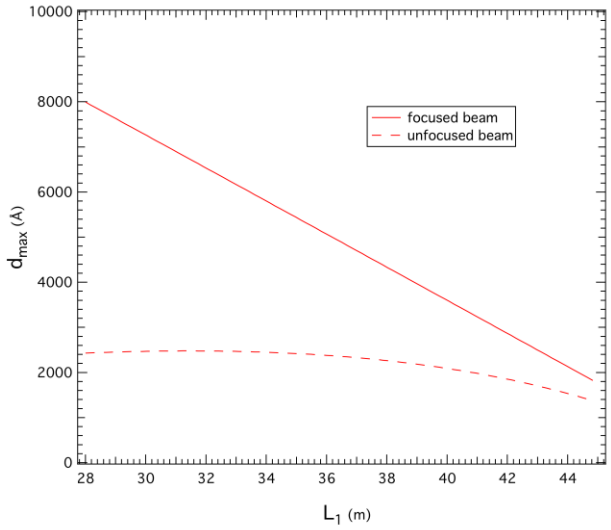

Figure 18: Maximum d-spacing in the vertical direction for a focused and unfocused beamline as a function of L_1 using a 2 mm aperture for d_2 and a vertical source size of 4 µm. In the horizontal direction

A further consideration is that of the angular resolution that can be achieved. For the focused beamline scenario the resolution, $\Delta\theta$, is determined by the size of the focal spot at the detector. In the case of the unfocused setup the angular resolution is determined by the divergence of the radiation. For the focused beamline scenario the angular resolution, $\Delta\theta$, is determined by the size of the focal spot Δ_d at the detector.

$$\Delta\theta \approx \frac{F_2}{F_1}.\frac{\Delta_d}{L_D}$$

Thus achieving a high angular resolution would require a large value of L_1. In practise only a small range of values for L_1 is accessible: 28 – 45 m corresponding to the space available in the optics hutch since no optical component is allowed in the front-end on the other side of the shield wall.

Currently BM26B has three apertures called H4, H5 and H6 where H4 should play the role of d_2 and H6 acting as d_3. The role of H5 is to give some flexibility to vary L_1 it could also act as a further guard slit although theoretically not significant.

Several SAXS beamlines have reported the benefit of single crystal slit blades for the beam defining slits and commercial solutions are available (JJ X-ray).

Any scatter from the slits close to the sample would give rise to a pronounced background at the detector and it would make sense to consider the use of a small aperture *just down stream* of the sample which is able to remove this parasitic contribution.

4.9 Filters

➔ *It is proposed to have two motorised racks with four to five slots that contain all the filters in a water-cooled support in a location upstream of the collimating mirror.*

The use of a water-cooled filter rack is very helpful in various circumstances and a relatively simple device to install. Together with the use of x-ray mirrors with different coatings a very effective energy filter is realised that helps to keep heat load on optical components down and reduces higher harmonics

from reaching the sample. Ideally the filters are made of different materials and thicknesses so that the beam can be attenuated by well-known factors. Materials suitable for filters include: Aluminium, graphite, glassy graphite (Sigradur K & G – www.htw-germany.com), CVD diamond (www.cvd-diamond.com).

Figure 16 shows the available flux as a function of energy for different combinations of mirrors (all at 4.5 mrad) and/or filters in order to limit the transmitted spectrum. For all calculations we used aperture size of 1x0.1 mrad^2 (*hxv*). Please note that only a single mirror reflection was used in the calculations.

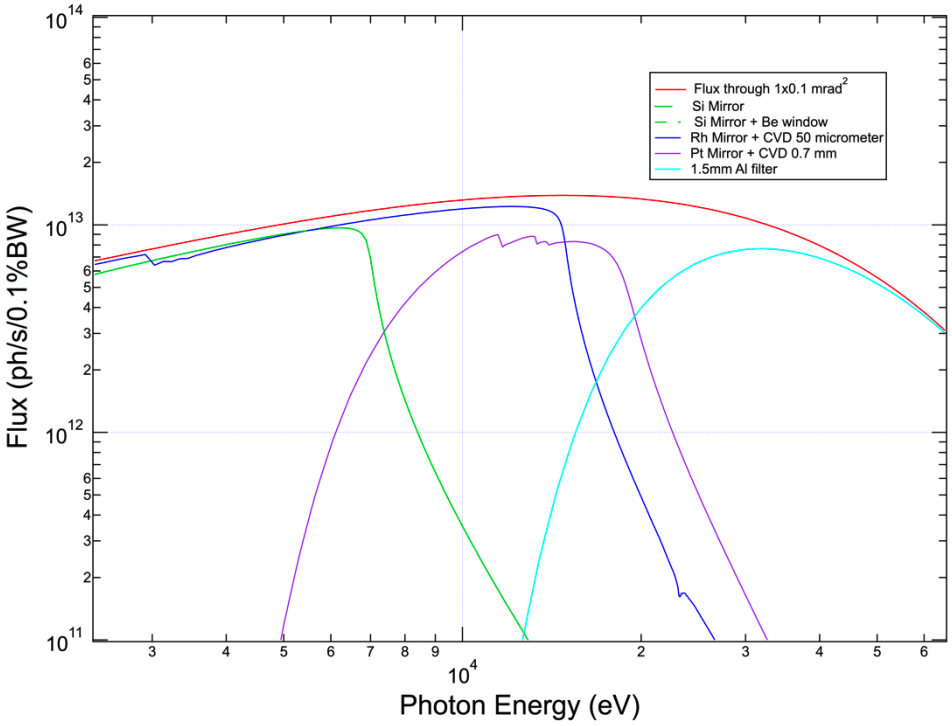

Figure 16: Expected flux at the sample for a white beam aperture of 1x0.1 mrad^2. Various filters and mirror coating combinations can be used to filter away particular energy ranges, which is helpful for reducing harmonics and heat loading. Only a single mirror reflection was used in the calculation and the angle of incidence was 4.5 mrad for all cases.

As part of the filter rack it is proposed to also install a wavefront pinhole array. This consists of a high-density material sheet with an array of pinholes. Each pinhole will produce a pencil beam that can be recorded downstream to observe the performance of key optical elements (see also diagnostics).

4.10 Additional Optical Components

A beamline is only as good as its optical components. Due to the fact that BM26 has a large optics hutch there is space available for future beamline upgrades.

One such option was already mentioned earlier: a multilayer monochromator. Such a device would allow up to two orders of magnitude more flux delivered at the sample due to the larger bandwidth of approx. 1%. In principle it is possible to have a so-called DMM in which the photon energy can be changed but in a smaller range than is available for the DCM. Furthermore, sagittal focusing is an option but requires a detailed design study. Having two monochromator setups in series is not a problem provided provisions are made to allow the white beam to travel through unhindered. There are two options regarding the installation of the DMM. It could be housed in the existing BM26A mono vessel that is available once that beamline moves away to another bending magnet port. Alternatively, the

DMM multilayer substrates could be attached to the two DCM crystals and thus re-using the DCM axes and vacuum vessel.

Another extension would be to control polarisation of the provided x-ray beam. Such an option will be of great benefit to investigations of chiral substances (practically all bio-materials) and magnetic materials. The required extra items are very modest and can be installed in a small vacuum chamber in the optics hutch.

By embracing a forward looking stance in the initial design and placement of beamline vacuum components such upgrades can be made quick and simple if and when needed.

5. Cooling of optical components

The optical elements exposed directly to the white beam need cooling to preserve the brilliance of the source. The total flux is the same as compared to the current situation and is concentrated in a horizontal fan that is identical as before resulting in a total flux of less than 500 W when integrated over all photon energies. In the new scheme the monochromator will be slightly closer to the source. By employing the right combination of collimating mirror coating and angle of incidence unwanted higher photon energies are removed (see figure 17) when the beamline is setup to select low photon energies, whereas filters can be helpful to cut lower energetic photon in the opposite case. We have performed some examples of expected power loading which correspond to some extreme examples in which the loading of the monochromator is particularly high. Once thermal distortions lead to slope errors equal to a significant fraction of the crystal acceptance angle a significant reduction in monochromatic flux levels will be evident.

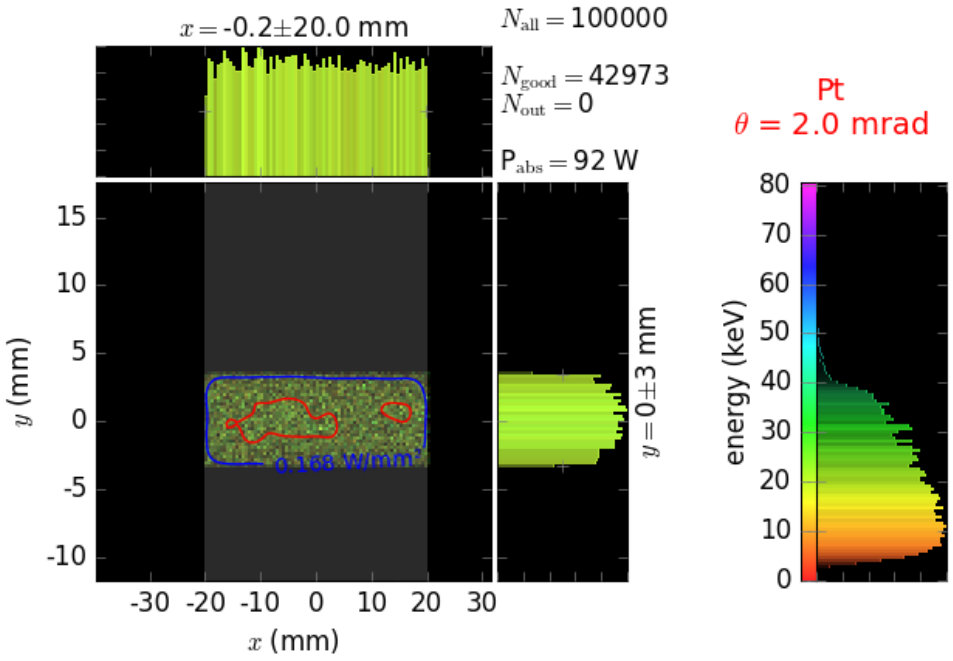

Figure 17: Ray trace results for heat load on first DCM crystal for 5 keV setting. The vertical collimating mirror (VCM) has at Pt coating and set at an incidence angle of 2 mrad. The contour levels are at 50% (blue) and 90% (red) of the highest power density. Note that the incident photon energy spectrum is shown on the right hand side.

Whilst it is unavoidable to have temperature differences, a good cooling scheme can minimise these. Typically direct water-cooling can be used at a power density of up to approx. 1 W/mm^2. For the SBM beamline we expect less than half of this value and thus an efficient directly water-cooled monochromator will work avoiding issues with complicated alternative cooling methods.

6. Diagnostics

Beam diagnostics will be of great benefit to smooth beamline operation and quality of beam provision to the users. Energy scans require multiple motor scans to keep the beam at a fixed height. Large changes in energy will, in addition to the DCM adjustments, require tilt and mirror coating changes. Availability of diagnostics enables a high level of automation of beamline operations. The use of in situ diagnostics is, however, to be limited due to the fact that most devices will introduce some increase in background scattering. Adding actuators to allow selective insertion of devices would provide complete flexibility.

- The following parameters should be monitored:
- White beam position upstream of VCM
- Intensity downstream of DCM
- Beam position/Intensity upstream of sample position
- Wavefront monitor
- Fluorescence screens/slits with fluorescence strips
- High resolution beam imager
- Knife edge scanning stage

Measurement of the beam position at several points along the beamline facilitates automatic alignment of key optical components. An intensity monitor placed at the exit of the DCM is a very useful option and can provide a control input into an automatic monochromator stabilisation system. A prototype system has been installed at BM26B and integration into the beamline system is underway.

A wavefront monitor consisting of a water-cooled micro pinhole array that can be inserted just upstream of the VCM is a very useful tool to diagnose whether the beam is properly collimated or whether any of the optical components suffer from misalignment. By recording the array of pencil-like beams at various points along the beamlne, an accurate recording is made of the wavefront as it travels down the beamline allowing traditionally tricky optimal bending of mirrors to be monitored much better. With a suitable placement of the pinholes such a device would also be able to act as a coherent fraction indicator using a traditional Young's slit measurement.
Another solution to measure the wavefront of the beam is to use a grating interferometer that uses a 2D or chessboard pattern. This approach has been used to measure thermal bumps on optical components [6]. Investing into these approaches of measuring beam quality are important if one wants to maintain brilliance of the beam.

A portable knife-edge scanner using a piezo stage is particularly useful to measure micrometre -sized beams at the sample position that are possible with the upgraded source and beamline. The anticipated size will be too small to be reliably captured by other means.

For accurate white beam power measurements it is helpful to have a calorimeter (isolated copper block with thermocouple) that can be moved into the beam for a brief period. Such measurements allow us to establish whether front-end equipment is well aligned

7. End station

The large existing SAXS/WAXS experiments hutch has benefitted from continuous updates and improvements both in terms of sample stages/environments and post-focusing optics. As such it is very easy to adapt the setup further to allow new sample environments, measurement geometries and detectors to be housed. As such the current end station supports a large range of experiments and it is anticipated that this flexibility is kept.

This flexibility allows experiments beyond small and wide-angle scattering. For example, one could implement several (combined) methods such as imaging or tomography but especially phase contrast imaging in which a significant free space path is needed down stream of the sample.

One proposed change is to support grazing incidence experiments by relocating the little used diffractometer that is currently located at the end of the hutch to the sample position. In this position a flexible sample stage and wide-angle detector mount is available. A newly acquired hexapod would act as the sample support at the centre of the diffractometer. For large and heavy setups the main cradle of the diffractometer would be able to handle sample environments over 500 kg. Nevertheless, there will still be large setups that can't be accommodated this way and for these there will be a dedicated space available downstream of the diffractometer. For that particular case the beam pipe will be extended thus avoiding air scattering as much as possible.

Micro- or post-focusing devices are envisaged to play an important role in increasing spatial resolution of the beamline. Certainly for KB-type microfocusing the location of such optics should be located close to the sample that, for BM26B, means in the experiments hutch. The current arrangement of swapping microfocusing optics in or out of the beam is rather poor and takes a large amount of space and is time consuming to setup. The setup should be changed such that these components can be permanently installed into the beamline (vacuum) such that they can still be removed from the beam fully remotely controlled without breaking vacuum. If this is not possible then an arrangement with a common kinematic mount is preferred over the current method that takes significant space. The optical element closest to the sample should be the KB mirrors enabling the smallest beam size at the sample. Whatever option is taken care should be taken to have end of beamline slits located close to the sample. A fast experiments shutter should be available that can be triggered using a unified and programmable trigger system that is able to trigger various pieces of equipment including sample environments.

8. Beamline Control, Data Acquisition and Data Analysis

Beamline control and operation software related is at the heart of beamline operations, get this wrong and beamline users come away with a bad experience or worse still with no data. Currently the beamline relies heavily on the availability and implementation of SPEC for both beamline and

experiments control something that was developed 20 years ago. At DUBBLE beamline and experiment control software development has been neglected for many years and has only recently had some progress with one dedicated member of staff and a specialist consultant.

Steps are being taken to adapt new control software to replace the current SPEC software. This is a serious programming effort and the options should be carefully weighed such that the result provides the best user experience. To rely on a series of SPEC macros to control the beamline is not particularly user friendly and requires a large documentation base and user effort to familiarise themselves with each control parameter. Efforts should be directed in creating a more intuitive way to select and control various settings. An attractive solution uses a beamline synoptic display, which gives a complete overview of all key beamline parameters such as beam intensity and vacuum pressures. Changing of key parameters would then be accomplished by interacting with objects on the synoptic that would bring up dedicated panels with all specific controls/readings. For more complex experiments which rely on hardware synchronisation a solution should be found to create an environment that allows easy configuration of experiment and data acquisition scheduling.

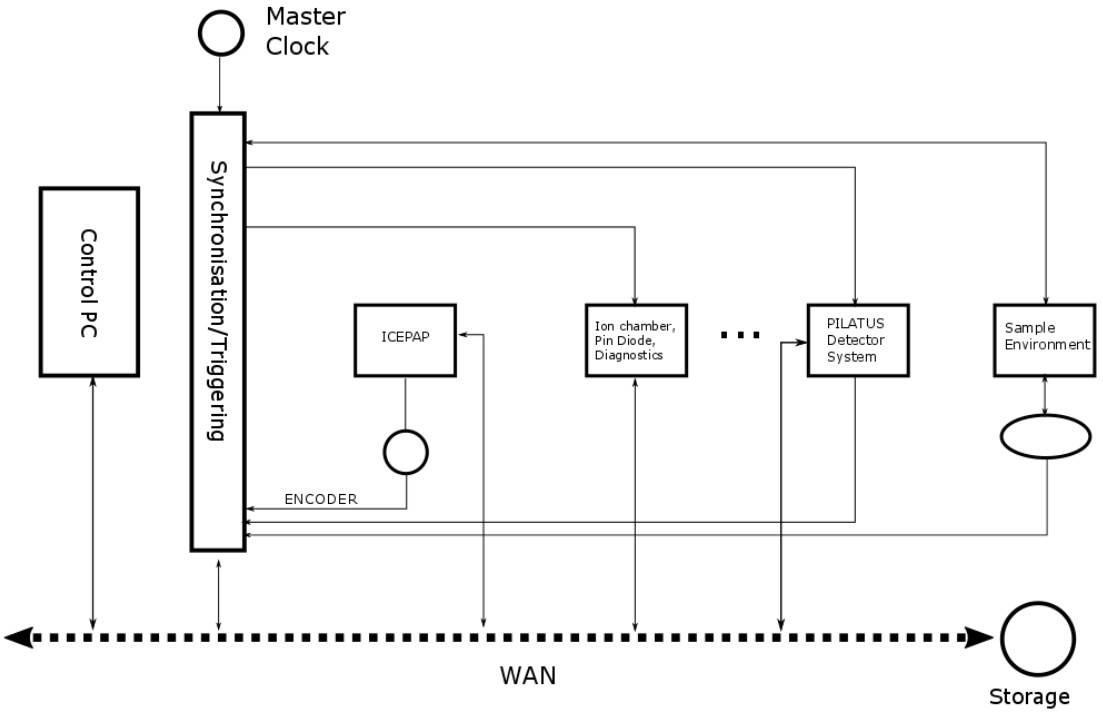

With the large variation of experiments conducted at this beamline a 'GDA'-like software will be a rather large software effort that ultimately won't offer the flexibility that is needed. It would be advisable to consider various options to allow easy use, on the one hand for fairly standard experiments, but also providing a more flexible approach through scripting of key tasks.

Irrespective of the status of the underlying, low-level control it is important that there is an inhouse software engineer to take responsibility to maintain and further develop the suite of software required by users particular on data acquisition but also on data analysis because it is important that acquired data is assessed on its quality shortly after measurements so that users can, at an early stage, have confidence in the quality of the data and plan their experiments optimally.

9. Detector requirements

The requirements for a high angular and time resolution, the beamline requires at least a fast hybrid photon counter that features small pixels covering a large area to cover a significant segment of *q*-space. As such the Dectris detectors are the golden standard in the field and with the Eiger family of detectors a good match is found with the above requirements reaching imaging rates of 500 Hz. The beamline currently has a state of the art 1M Pilatus 3 system capable of collecting frames at a rate of 30 Hz which can be upgraded to 300 Hz if and when required. A combination of the two systems would be advisable to make sure that if one system is down there is always a backup. The backup system could also be made available for use at the X-ray spectroscopy beamline if combined spectroscopy and small angle scattering is to be combined.

For simultaneous measurements of large scatter angles a dedicated Pilatus 300k system is available that will be suitable for the foreseeable future. For high resolution work there is a requirement for x-ray imaging detectors with a small pixel size. The standard Silicon photodiode layer isn't optimal for energies above 15 keV but tolerable until about 20 keV above this energy the use of GaAs or CdTe should be preferred.

The use of a large Kapton vacuum window at the end of the flight tube is not ideal. The use of a Dectris detector with a vacuum flange would overcome this issue but at a significant cost and some concern regarding protection of the detector is not amiss.

10. Conclusions

The presented beamline layout consists of a well-proven concept in which focusing elements are separated from elements that select photon energy. Through the use of collimating mirror and selected filter materials of the full source spectrum can be restricted such that the monochromator heat load is minimised. Monochromator cooling should be improved by copying the multi-bore directly cooled crystals such as currently used in the new BM26A monochromator.

Comparing the key parameters before and after the shutdown it becomes clear that the joint upgrade of radiation source and beamline provides real benefit to the users and unlocks new techniques that can be combined with the existing ones. Higher flux (2 - 10x) is due to reduced thermal distortions and larger fan acceptance of the new optics. With the multi-layer monochromator improvements of over two orders of magnitude will be reached. Together with the boost in brilliance the new beamline transform the types of experiments that are currently difficult or impossible to do.

Ray trace studies have highlighted the requirement for sub-microradian slope errors for collimating and focusing mirrors when source brilliance is to be maintained. In the current setup there was no space for a collimating mirror, the new setup should include a VCM if it were only for reduction of the heat load onto the monochromator. Also mirror bending mechanisms and gravity compensating mirror mounts are important for maintaining source brilliance. For intermediate energies the use of Rhodium coating is preferred to that of Platinum due to the higher reflectivity of Rh at these energies.

Similarity of the proposed beamline concept with the existing BM26B beamline will enable reuse of many components such as slits, vacuum vessels, support structures and vacuum pumps. Beamline electronics such as motor drives have had the benefit of recent upgrades.

Reusing the BM26A hutch by the use of a transparent monochromator provides scope to introduce a new facility at a very low cost since it will be using existing hutches and infrastructure.

Key beam defining components (mirrors, DCM, slits and diagnostics) will require stable mounting removing as much as possible box steel frames.

A technical design report will detail the various cost/performance options available based on this concept report together with user requirements.

11. References

[1] K. Klementiev and R. Chernikov, (2014) Proc. of SPIE Vol. 9209 92090A-1 (doi: 10.1117/12.2061400).

[2] J. Chavanne, ESRF document 01#15/IDM/ version 0, unpublished (2015).

[3] I.K. Robinson, Z. Kristallogr. Suppl. (2008) **27**, 27-35 (doi:10.1524/zksu.2009.0005).

[4] G. B. M. Vaughan, J. P. Wright, A. Bytchkov, M. Rossat, H. Gleyzolle, I. Snigireva, and A. Snigirev, J. of Synchrotron Rad. (2011) **18**, 125-133.

[5] IDT document DUB-105-65-01 iss3, FEA report of DUBBLE DCM first crystal.

[6] S. Rutishauser *et al.,* J. Synchrotron Rad. (2013) **20**, 300-305 (doi:10.1107/S0909049513001817).